CrossMark

Copper indium gallium disulphide (CuInGaS$_2$) thin films deposited by spray pyrolysis for solar cells: influence of deposition time in controlling properties of sprayed CuInGaS$_2$ absorbers

Ahmed Kotbi[1,2] · Bouchaib Hartiti[1] · Salah Fadili[1] ·
Abderraouf Ridah[2] · Philippe Thevenin[3]

Abstract CuInGaS$_2$ (CIGS) multi-component semiconductors thin films were elaborated by spray pyrolysis on glass substrates using different spray times. The structural, optical and electrical properties of CuInGaS$_2$ thin films were investigated. The obtained films were characterized using X-ray diffraction, Raman spectroscopy (RS), UV–Vis spectrophotometer and Hall Effect measurement. Thin films were formed by varying deposition time in the range, 30–50 min, keeping other deposition parameters as constant. The X-ray spectra revealed that the CuInGaS$_2$ thin films have chalcopyrite structures with a highly (112) preferential orientation. The best crystallinity is obtained for HK-50 the maximum (112) peak intensity. RS also confirmed this structure. Optical constants such as band gap (E$_g$), extinction coefficient (k), refractive index (n), dielectric constants (ε_r) and (ε_i) and optical conductivity (σ_{opt}) were calculated from the measured transmittance and absorption spectra in the wavelength range between 550 and 900 nm. The bulk concentration, mobility (μ), conductivity (σ), resistivity (ρ) and conduction type of thin films obtained at different deposition times were determined using Hall Effect measurements. It has been observed that the optimum time of spray was 50 min for best performed CuInGaS$_2$ thin films with low resistivity and high mobility. Deposition time has been discussed to obtain the high quality thin film absorbers for solar cell applications. Here, we report a study on structural, optical and electrical properties of CuInGaS$_2$ films grown by chemical spray pyrolysis in view of its application as an absorber in thin film solar cells.

✉ Ahmed Kotbi
kotbi.ahmed7@gmail.com

1 MAC&PM Laboratory, ANEPMAER Group, FSTM, Hassan II Casablanca University,
   B.P 146, Mohammedia, Morocco

2 LIMAT Laboratory, Department of Physics, FSB, Hassan II Casablanca University,
   B.P 7955, Casablanca, Morocco

3 LMOPS Laboratory, Department of Physics, University of Lorraine, Metz, France

1 Introduction

$CuInSe_2$, $CuInS_2$, $CuInGaSe_2$, $CuInGaS_2$ and $CuZnSnS_4$ semiconductors have been the focus of intense studies as photoabsorber layers in thin film solar cells. Among them, $CuInS_2$ is one of the most important materials due to its optimum band gap energy of $E_g = 1.5$ eV (Kamoun et al. 1994; Mahendran and Suriyanarayanan 2013; Rafi et al. 2012), a high absorption coefficient ($\alpha > 10^4$ cm^{-1}) and good p- or n-type conductivity (Ernst et al. 2003). In the past few years, various methods for the deposition of $CuInS_2$ chalcopyrite semiconductors onto substrates have been reported, such as electrodeposition (Yukawa et al. 1996), chemical bath deposition (Mahmoud and Eid 1997; Pathan and Lokhande 2004), sol-gel dip coating (Aslan et al. 2013), metal-organic decomposition (Nakamura and Ando 2005) and chemical spray pyrolysis (Caglar et al. 2008; Santhosh et al. 2014; Krunks et al. 2006). For economical reasons, it will be useful to prepare thin films using a low cost deposition technique. One of such methods is a spray pyrolysis technique, which allows to obtain large area films at extremely low cost. In several studies it was shown that the physical properties of $CuInS_2$ thin films could be improved by optimized deposition conditions (Vadivel et al. 2013) and doping. For controlling a conduction type and obtaining a low resistivity, several impurities doped $CuInS_2$ thin films such as aluminum (Al) (Cheng and Fan 2013), sodium (Na) (Zribi and Kanzari 2011), antimony (Sb) (Akaki et al. 2003), Zinc (Zn) (Ben Rabeh and Kanzari 2011) and Gallium (Ga) (Aydin et al. 2014; Ajili et al. 2014; Kim and Kim 2012) have been also studied. However, there is very limited information in literature about spray pyrolysis of $CuInGaS_2$ absorbers. In this work, The effect of deposition time on the structural, optical and electrical properties of $CuInGaS_2$ thin films is reported.

2 Experimental details

In the present work, $CuInGaS_2$ thin films were deposited on glass substrates employing chemical spray pyrolysis technique in which the precursor solution was prepared using cupric chloride ($CuCl_2$), indium trichloride ($InCl_3$), gallium trichloride ($GaCl_3$) and thiourea ($CS(NH_2)_2$) and compressed air was the carrier gas. Before deposition, the substrates were chemically cleaned with dilute nitric acid and ethanol. The aqueous solutions used for pulverization contain the precursors of the $CuInS_2$ material, i.e. 1.1×10^{-2} M of $CuCl_2$ for the copper, 1×10^{-2} M of $InCl_3$ for the indium and 4×10^{-2} M of ($CS(NH_2)_2$) for the sulfur. The $CuInS_2$ films were formed by the following reaction:

$$CuCl + InCl_3 + 2SC(NH_2)_2 + 4H_2O \Rightarrow CuInS_2 + 2CO_2 + 4NH_4Cl \qquad (1)$$
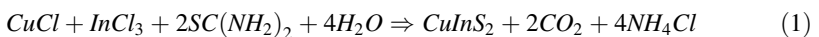
The gallium trichloride $GaCl_3$ (1.5×10^{-3} M) is added to the starting solution to obtain $CuInGaS_2$ thin films. $CuInGaS_2$ thin films were prepared using different times of spray 30, 40 and 50 min, keeping all other parameters constant. The spray rate was 1.6 mL/mim. The distance between spray head and substrate was maintained at 30 cm. Substrate temperature was kept constant at 375 °C during all experiments.

The thicknesses of $CuInGaS_2$ films were estimated to be between 1.83 μm and 1,99 μm. The determination of the crystallinity and orientation of the deposits was made by X-ray diffraction using a diffractometer with a copper source whose Kα emission ray has a wavelength equal to 0.154 nm. The X-ray diffraction (XRD) patterns of $CuInGaS_2$ samples were recorded in the 2θ range of 10° to 80°. The crystal structure of the films was confirmed by Raman Spectra (RS). The optical absorption and transmittance spectra were

recorded in wavelength range of 450–900 nm by spectrophotometric. The bulk concentration, mobility (μ), resistivity (ρ), conductivity (σ) and conduction type of thin films were determined using Hall Effect measurements.

3 Result and discussions

3.1 Structural studies

X-ray diffractograms of CuInGaS$_2$ thin films deposited at different spray times are depicted in Fig. 1. The diffraction peaks at 27.97°, 46.78° and 55.14° correspond to the (112), (220)/204) and (312)/(116) crystal planes of the tetragonal CuInGaS$_2$ phase. No peaks corresponding to secondary phases were observed in the diffractogram. All samples were polycrystalline in nature. The intensity of (112) peak corresponding to CuInGaS$_2$ increased with deposition time. Increase in spray time leads to increase in size of crystallites as observed from the sharpening of the X-ray diffraction peaks. In Table 1 are listed the various rations I(204)/I(112) and I(312)/I(112) determined from the X-ray diffraction spectra. From the Table 1 it is clear that the minimum ratios are obtained for HK-50 and all ratios of relative intensities are much less than 1. Thus, we can confirm that CuInGaS$_2$ thin films were preferentially oriented towards the direction (112). Determination of grain size from X-ray diffractograms showed that even the best crystalline films (HK-50) had a grain size of only D= 5.55 nm which indicates the nanocrystalline nature. The grain size of samples can be calculated using Scherrer's equation (Warren 1990):

$$D = \frac{k\lambda}{\beta cos\theta} \tag{2}$$

where D is the grain sizes of samples, k is the shape factor which usually takes value of 0.94, λ is the wavelength of the CuK$_\alpha$ radiation (0.154 nm), β is the line boarding at half
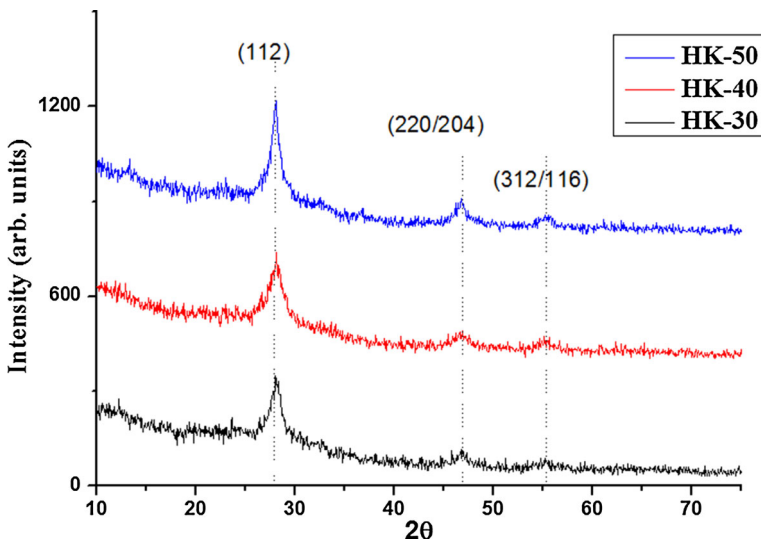
Fig. 1 XRD patterns of CuInGaS$_2$ films deposited at different times of spray

Sample name	I(204)/I(112)	I(312)/I(112)
HK-30	0.32	0.25
HK-40	0.31	0.27
HK-50	0.30	0.21

the maximum intensity, and θ is the Bragg angle. The grain sizes estimated from Scherrer's formula are in the range 3.02–5.55 nm as shown in Table 2. The maximum value is obtained for CuInGaS$_2$ thin films deposited at 50 min. The increase of the grain size can be explained by an improvement of the crystallinity. Using grain size values, the dislocation density (δ), defined as the length of dislocation lines per unit volume of the crystal has been calculated by using the Williamson and Smallman's formula (Warren 1990):

$$\delta = \frac{1}{D^2} \tag{3}$$

Table 2 shows the variation of the dislocation density δ and the lattice strain as a function of the deposition time. It is clear that δ decreases from 10.96×10^{10} to 3.246×10^{10} lines mm^{-2}. The reduction in the dislocation density and the lattice strain with increase of deposition time was probably due to the stress relaxation, which was observed during the recrystallization process. Similar result was reported by Ajili et al. (2014).

Raman spectroscopy is a standard characterization technique to indicate the exact phases of quaternary semiconductor compound thin films. The Fig. 2 presents the Raman spectra of the samples deposited at different spray times in the wavelength range 200–600 cm^{-1}. The Raman spectra contains modes at 240 cm^{-1}, 295 cm^{-1} and 340 cm^{-1}. These modes are characteristic vibration symmetry of the tetragonal phase of CuInGaS$_2$ thin films. The Raman shifts near 240, 295 and 340 cm^{-1} are presumably belonging to E$_{TO}^3$, A$_{LO}^1$ and E$_{LO}^1$ modes of the CH-ordering of chalcopyrite phase (Lee and Kim 2010).

3.2 Optical properties

Figure 3a, b shows the optical transmittance T(λ) and absorbance A(λ) spectra respectively of CuInGaS$_2$ films in the wavelength range 450–900 nm. The absorption coefficient (α) of CuInGaS$_2$ films (Fig. 3c) was evaluated from the transmittance data by using the following relation (Koschel and Bettini 1975; Majeed Khan et al. 2011):

Table 2 Some structural properties of CuInGaS$_2$ thin films

Sample name	Time of spray (min)	Grain size (nm)	The dislocation density δ ($\times 10^{10}$ lines mm^{-2})	Lattice strain
HK-30	30	3.02	10.96	0.0496
HK-40	40	3.32	9.072	0.0451
HK-50	50	5.55	3.246	0.0270

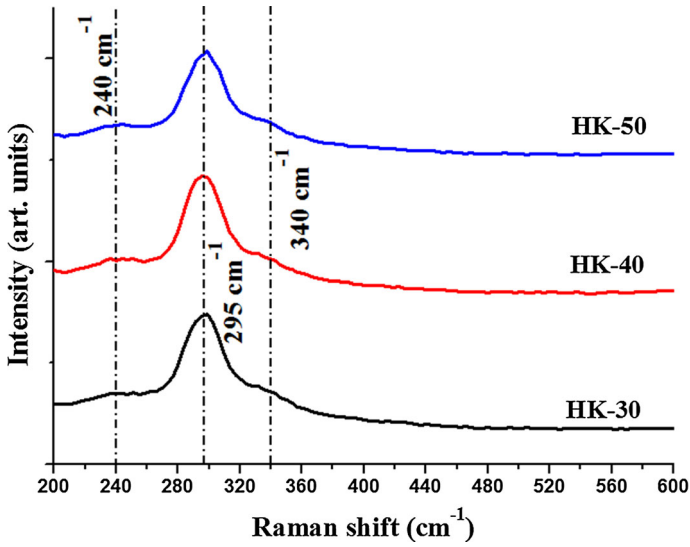**Fig. 2** Raman scattering measurements of CuInGaS$_2$ sprayed thin films
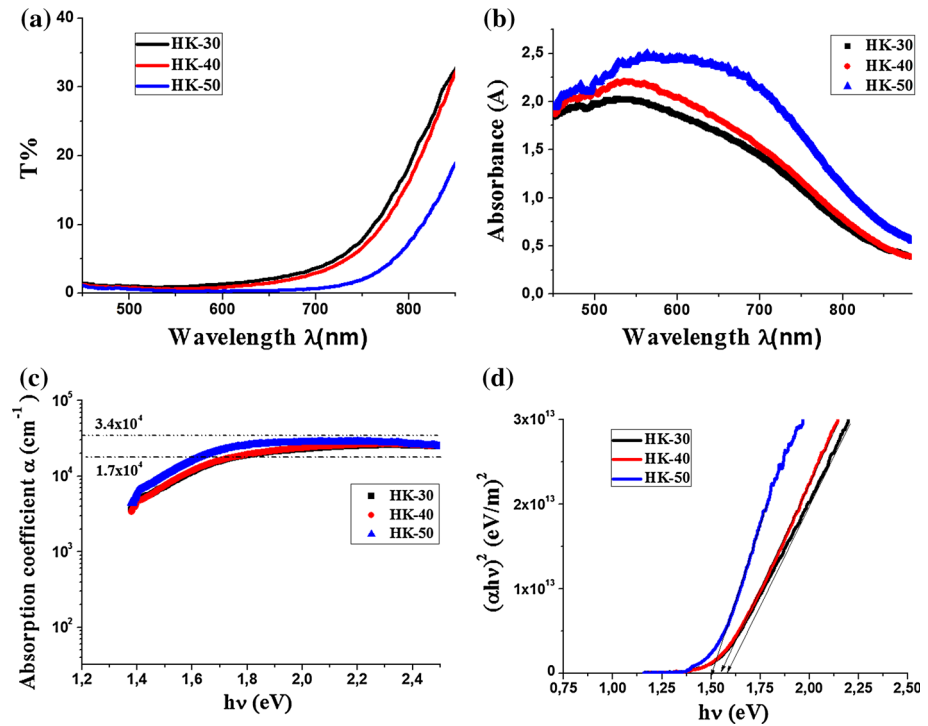
Fig. 3 a Optical transmittance and **b** absorbance spectra of CuInGaS$_2$ thin films. **c** Absorption coefficient (α) and **d** $(\alpha h\nu)^2$ versus photon energy for CuInGaS$_2$ thin films prepared at 30, 40 and 50 min

$$\alpha = \frac{1}{d} ln\left(\frac{1}{T}\right) \tag{4}$$

where d is the film thickness. It is apparent from Fig. 3c that the absorption coefficient increases suddenly and presents a maximum value around $3.4 \times 10^4\, cm^{-1}$ in the visible range 1.4–2.5 eV, which is important for the increase of the photovoltaic efficiency in solar cells. The maximum value of the absorption coefficient is found for the samples prepared at 50 min. We note that the absorption coefficient of $CuInGaS_2$ thin films moved to greater energies when the deposition time increases.

The optical band gap (E_g) can be found from the calculated values of the absorption coefficient, it should be pointed out that the absorption coefficient of crystallized semi-conductors, in the high absorption region ($>10^4\, cm^{-1}$) is given according to the model proposed by Tauc and Menth (1972) and Pankove (1971), by the expression relating the absorption coefficient (α) to the photon energy ($h\nu$):

$$\alpha h\nu = A(h\nu - E_g)^m \tag{5}$$

where A is a constant and m is an exponent that characterizes the optical absorption process (m = 1/2 for direct allowed transition and m = 2 for indirect allowed transition). Plotting of $(\alpha h\nu)^2$ versus photon energy ($h\nu$), yields a straight line indicating a direct optical transition as showed in Fig. 3d. The values of the optical band gaps of $CuInGaS_2$ films are listed in Table 3. The observed band gap value for HK-50 (1.50 eV) is the theoretical band gap value of $CuInGaS_2$ thin films. The band gap of 1.50 eV for an absorber layer is beneficial in improving the efficiency of the cell. A correlation has been found between time of spray and band gap. Table 3 shows a decrease in the values of the direct energy gap of $CuInGaS_2$ thin films by increasing the deposition time. In the semiconductors, several possible reasons that contribute to a decrease in band gaps have been postulated (Yeh and Cheng 2015). In the present study, the decrease of optical band gap could be attributed to two factors. Indeed, it may be attributed to the improvement of crystallinity and the increase in the grain size caused by increasing the deposition time (Ghobadi 2013) this is confirmed by X-ray diffraction (XRD) or to the presence of unsaturated defects which increase the density of localized states in the band gap (Bakr et al. 2011).

The complex refractive index n*=n-ik, where n is the refractive index, and k is the extinction coefficient, which can be expressed in terms of the absorption coefficient (α) by the equation (Yakuphanoglu et al. 2004):

$$k = \frac{\alpha\lambda}{4\pi} \tag{6}$$

The reflectivity R, the refractive index n and the extinction coefficient k of crystalline solids are related through the equation (El-Korashy et al. 2003):

Table 3 The optical energy gap E_g for $CuInGaS_2$ at different deposition times

Sample name	Time of spray (min)	E_g (eV)
HK-30	30	1.57
HK-40	40	1.53
HK-50	50	1.50

$$n = \left(\frac{1+R}{1-R}\right) + \sqrt{\frac{4R}{(1-R)^2} - k^2} \qquad (7)$$

The transmittance T is related to its reflectivity R and absorption coefficient α through (Fox 2010):

$$T = (1-R)^2 exp(-\alpha d) \qquad (8)$$

We will derive the reflectivity R from eq. (8). Figure 4 shows the optical reflectivity calculated by the equation (9) of CuInGaS2 thin films:

$$R = 1 - \left(\frac{T}{exp(-\alpha d)}\right)^{1/2} \qquad (9)$$

Figure 5a, b present the refractive index (n) and the extinction coefficient (k) as a function of wavelength of the CuInGaS$_2$ thin films prepared with different deposition times. In one hand, the refractive index and extinction coefficient values decrease with increasing wavelength. Therefore, they show normal dispersion. On the other hand, the refractive index values and the extinction coefficients are influenced by the deposition time, and both of them increase with it. The slight increase in refractive index with increasing deposition time can be attributed to an increase in packing density. This is expected because the film porosity decreases with increasing deposition time. Table 4 shows the dependence of k and n on wavelength for all the investigated films.

Other way, if the refractive index and the extinction coefficient are known, the real and imaginary parts of dielectric constant of the film can be also estimated. The real and imaginary parts of complex dielectric constant can be expressed as (Hodgson 1970):

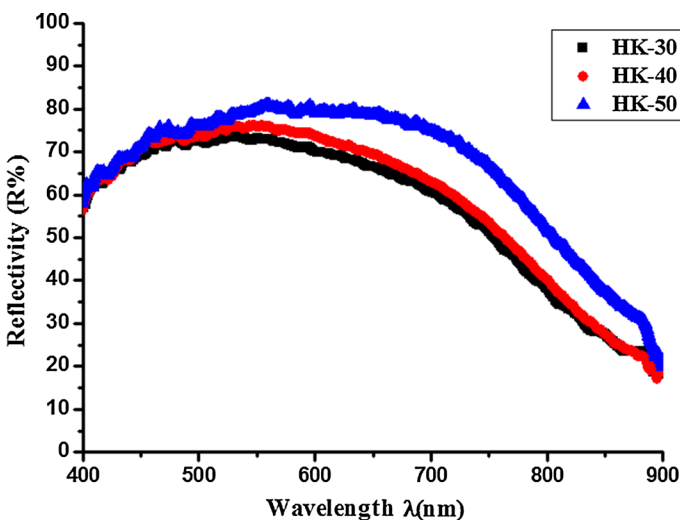$$\varepsilon_r = n^2 - k^2 \qquad (10)$$

Fig. 4 Variation of reflectivity R with wavelength for CuInGaS$_2$ layers
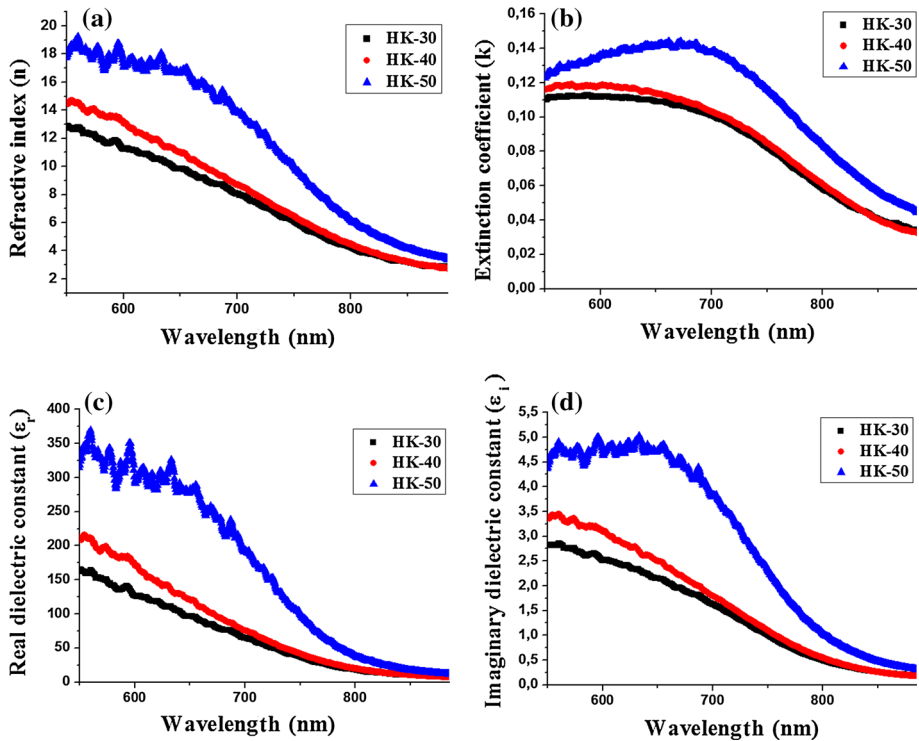
Fig. 5 The variation of **a** refractive index, **b** extinction coefficient, **c** real and **d** imaginary part of the dielectric constants with wavelength at different deposition times for CuInGaS$_2$ films

Table 4 Refractive index n, extinction coefficient k, the real ε_r and imaginary ε_i dielectric constants and optical conductivity (σ_{opt}) for CuInGaS$_2$ at different deposition times (at $\lambda = 835$ nm)

Sample name	Time of spray (min)	n	k	ε_r	ε_i	σ_{opt}
HK-30	30	3.32	0.0454	11.04	0.30	5.42×10^{13}
HK-40	40	3.47	0.0456	12.09	0.31	5.70×10^{13}
HK-50	50	4.66	0.0639	21.74	0.59	1.07×10^{14}

$$\varepsilon_i = 2nk \tag{11}$$

The variation of both real and imaginary dielectric constants (ε_r and ε_i) with wavelength are shown in Fig. 5c, d. The real and imaginary parts follow the same pattern and it is seen that the values of real part are higher than the imaginary parts.

Optical response of a material is most conveniently studied in terms of optical conductivity. The optical conductivity (σ_{opt}) has been determined from the relation (Gedi et al. 2015):

$$\sigma_{opt} = \frac{\alpha n c}{4\pi} \tag{12}$$

where α is the absorption coefficient, c is the velocity of light and n is the refractive index. The optical conductivity directly depends on the absorption coefficient and the refractive
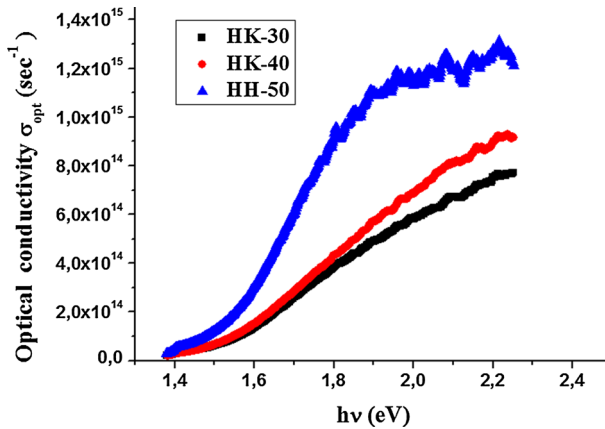
**Fig. 6** Variation σ_{opt} with $h\nu$ for CuInGaS$_2$ layers

index is found to increase sharply for high energy values due to large absorption coefficient and refractive index. The plots of optical conductivity (σ_{opt}) as a function of photon energy for as-grown CuInGaS$_2$ layers are shown in Fig. 6. It shows that optical conductivity (σ_{opt}) increases with an increase of photon energy ($h\nu$) as well as bath deposition time up to the optimum value (50 min). The increase of optical conductivity (σ_{opt}) may be attributed to the increase of both absorption coefficient (α) and refractive index (n) with deposition time and may also be due to the change in density of localized states in the band gap (Mott and Davis 1970), excitation of electrons by photon energy (Yakuphanoglu et al. 2005). The values of n, k, ε_r, ε_i and σ_{opt} at 835 nm wavelength are given in Table 4. A similar behaviour of variation of optical conductivity was also observed by Kotbi et al. (2016) in CuInS$_2$ films.

3.3 Electrical properties

Electrical properties of the CuInGaS$_2$ films deposited on glass substrate at different spray times are studied using Hall measurement technique at room temperature. The bulk concentration, mobility, conductivity, resistivity and conduction type of thin films were determined. As it is seen from Table 5, all films showed p-type conductivity. It is apparent also from Fig. 7 that the mobility (μ) increased with increasing the deposition time from 30 to 50 min. Maximum electrical mobility of 1.42 cm^2/V s was observed for the sample prepared at 50 min. The resistivity of the samples revealed that film prepared at 50 min was less resistive than the other samples. This result can be explained by the good crystallization of CuInGaS$_2$ thin layers, which is confirmed by X-ray diffraction (XRD). The bulk concentration, resistivity and conductivity of HK-50 are 1.50×10^{20} cm^{-3}, 2.91×10^{-2} Ω cm and 34.29 Ω^{-1}cm^{-1} respectively. We can refer the high values of carrier concentration, probably to the fact that the material contains defects related to the preparation conditions, and the method used in the synthesis that could directly affect the bulk concentration. Otherwise, the low resistivity of the sample HK-50 can be ascribed to the higher crystallite size (Sharma and Rajaram 2010). Since the resistivity is related to the concentration of majority carriers in the film by the relationship $\rho = 1/e\mu N$ (Gedi et al. 2015), where N is the carrier concentration, μ is the mobility, 'e' is the electronic charge and ρ is

Table 5 Electrical properties of thin films obtained at different deposition times

Name	Time (min)	Bulk concentration (1/cm^3)	Resistivity (Ω cm)	Conductivity (1/Ω cm)	Mobility (cm^2/V s)	Type
HK-30	30	4.4593E+20	3.8747E−2	2.5808E+1	3.6126E−1	p
HK-40	40	1.0772E+20	4.8236E−2	2.0731E+1	1.2013E+0	p
HK-50	50	1.5067E+20	2.9161E−2	3.4292E+1	1.4206E+0	p
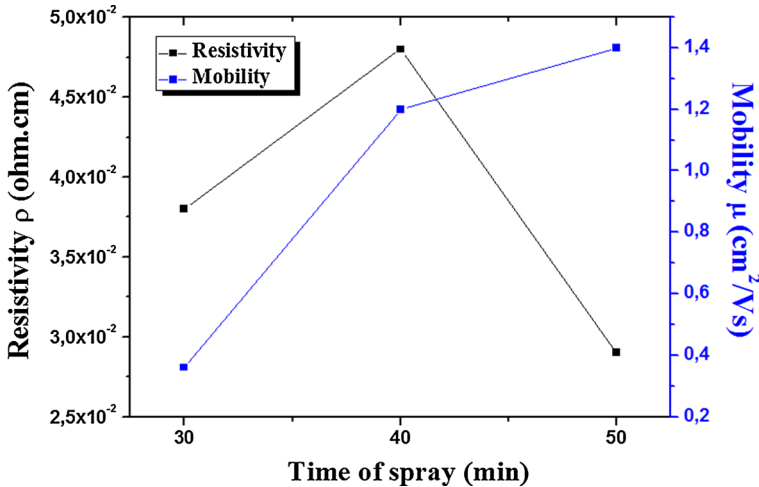
Fig. 7 Variation of the resistivity and mobility of CuInGaS$_2$ sprayed thin films

the resistivity, so low resistivity means a large carrier concentration. Similar carrier concentration values are reported for CuInS$_2$ films prepared by sulfurization (Cheng et al. 2013), Cu$_2$ZnSnS$_4$ films prepared by electro-deposition (Tang et al. 2016) and Cu$_2$SnS$_3$ thin films absorbers by co-evaporation (Srinivasa Reddy et al. 2015). The carrier densities up to 10^{21} cm^{-3} have been reported in the literature (Unveroglu and Zangari 2015). Generally, the electrical properties of I-III-VI$_2$ samples can be adjusted with small deviations from stoichiometry in the crystal (Hattori et al. 1992). The variation of [2S]/[Cu + 3(In+Ga)] − 1 ratios in samples is related to the conduction type of samples (Bandyopadhyaya et al. 2000). The non-stoichiometry parameter (Δy=[2S/(Cu+3(In+Ga))] − 1) almost constant, since all the deposition conditions are fixed except the deposition duration. The deposition duration has no influence on the final concentration of the components of films but it has an influence on the thickness. Then the non-stoichiometry parameter Δy does not change. We have prepared the starting solution with an excess of sulfur, so the non-stoichiometry parameter will always be positive despite the variation of the deposition time. For all films $\Delta y = 0.75 > 0$ and sulfur can act as an acceptor, indicates p-type conductivity of the films (Xu et al. 2011). The Δy value calculated in the solution and results from Hall measurements are in good agreement. Moreover, the positive sign of Hall coefficient confirmed the p-type of conductivity for all samples. From the present study it is clear that the CuInGaS$_2$ films can be a potential absorber layer material for thin film solar cells.

4 Conclusion

In Summary, CuInGaS$_2$ thin films have been prepared by chemical spray pyrolysis method. The influence of spray time on various structural, optical and electrical properties of the films were investigated by means of X-ray diffraction (XRD), Raman scattering spectroscopy, UV–Vis spectrophotometer and Hall Effect measurement. It was observed that the film deposited at 50 min shows good quality Chalcopyrite structure of CuInGaS$_2$ with preferred orientation of (112), (220)/(204) and (312)/(116) planes as revealed by the XRD pattern. XRD data also used to calculate the grain size, the dislocation density and the lattice strain of the spray pyrolyzed CuInGaS$_2$ thin films. Structural studies by Raman spectra confirmed that the CuInGaS$_2$ thin films are of chalcopyrite crystalline phase. The band gap energy and optical parameters of thin film have been investigated by the measurement of optical absorbance and transmittance data as a function of wavelength. Optical transmission measurements in the wavelength range between 450 and 900 nm showed that band gap energy of CuInGaS$_2$ thin films was ranging between 1.50 and 1.57 eV depending on the deposition time. From this prepared condition (50min) we found an optimal band gap energy value of 1.5 eV for solar energy conversion. The minimum resistivity, $2.91 \times 10^{-2} \Omega$ cm, was observed for the films deposited on glass substrates at 50 min. The bulk concentration, conductivity and mobility are 1.50×10^{20} cm^{-3}, 34.29 Ω^{-1}cm^{-1} and 1.42 cm^2/ V s respectively. These studied properties will play an important role in the fabrication of CuInGaS$_2$ thin films.

References

Ajili, M., Castagné, M., Turki, N.K.: Characteristics of CuIn$_{1-x}$Ga$_x$S$_2$ thin films synthesized by chemical spray pyrolysis. J. Lumin. **150**, 1–7 (2014)

Akaki, Y., Komaki, H., Yokoyama, H., Yoshino, K., Maeda, K., Ikari, T.: Structural and optical characterization of Sb-doped CuInS$_2$ thin films grown by vacuum evaporation method. J. Phys. Chem. Solids **64**, 1863–1867 (2003)

Aslan, F., Zarbali, M.Z., Yesilata, B., Mutlu, J.H.: Effects of Cu/In ratio and annealing temperature on physical properties of dip-coated CuInS$_2$ thin films. Mater. Sci. Semicond. Process. **16**, 138–142 (2013)

Aydin, E., Sankir, M., Demirci, N.: Sankir, spray pyrolyzed copper indium gallium sulfide thin films. J. Alloys Compd. **615**, 461–468 (2014)

Bakr, N.A., Funde, A.M., Waman, V.S., Kamble, M.M., Hawaldar, R.R., Amalnerkar, D.P., Jadkar, S.R.: Determination of the optical parameters of a-Si: H thin films deposited by hot wire-chemical vapour deposition technique using transmission spectrum only. Pramana J. Phys. **76**, 519–531 (2011)

Bandyopadhyaya, S., Chaudhuri, S., Pal, A.K.: Synthesis of CuInS$_2$ films by sulphurization of Cu/In stacked elemental layers. Solar Energy Mater. Solar Cells **60**, 323–339 (2000)

Caglar, M., Ilican, S., Caglar, Y.: Structural, morphological and optical properties of CuAlS$_2$ films deposited by spray pyrolysis method. Opt. Commun. **281**, 1615–1624 (2008)

Cheng, K.-W., Yen-Ching, W., Yu-Tung, H.: Ternary CuInS$_2$ photoelectrodes created using the sulfurization of Cu–In metal precursors for photoelectrochemical applications. Mater. Res. Bull. **48**, 2457–2468 (2013)

Cheng, K.-W., Fan, Miao-Syuan: Preparation and characterization of CuIn$_x$Al$_{1-x}$S$_2$ films using the sulfurization of metal precursors for photoelectrochemical applications. J. Taiwan Inst. Chem. Eng. **44**, 407–414 (2013)

El-Korashy, A., El-Zahed, H., Radwan, M.: Optical studies of $(NH_4)_2SO_4$ single crystal in the paraelectric phase. J. Phys. Chem. Solids **64**, 2141–2146 (2003)

Ernst, K., Belaidi, A., Konenkamp, R.: Solar cell with extremely thin absorber on highly structured substrate. Semicond. Sci. Technol. **18**, 475–479 (2003)

Fox, M.: Optical Properties of Solids, pp. 366–367. Clarendon Press, Oxford (2010)

Gedi, S., Minnam Reddy, V.R., Park, C., Chan-Wook, J., Ramakrishna Reddy, K.T.: Comprehensive optical studies on SnS layers synthesized by chemical bath deposition. Opt. Mater. **42**, 468–475 (2015)

Gedi, S., Reddy, V.R.M., Park, C., Chan-Wook, J., Ramakrishna Reddy, K.T.: Comprehensive optical studies on SnS layers synthesized by chemical bath deposition. Opt. Mater. **42**, 468–475 (2015)

Ghobadi, N.: Band gap determination using absorption spectrum fitting procedure. Int. Nano Lett. **3**(2), 1–4 (2013)

Hattori, K., Akamatsu, K., Kamegashira, N.: Electrical properties of polycrystalline chalcopyrite $AgInS_2$ films. J. Appl. Phys. **71**, 3414–3418 (1992)

Hodgson, J.N.: Optical absorption and dispersion in Solids, 8-10. Chapman and hall LTD, 11 New fetter Lane London EC4 (1970)

Kamoun, N., Bennaceur, R., Frigerio, J.M.: Etude des proprits optiques des couches minces de $CuInS_2$ et d'In-S. J. Phys. III Fr. **4**, 983–996 (1994)

Khan, M.A.M., Kumar, S., Ahamed, M., Alrokayan, S.A., Alsalhi, M.S., Alhoshan, M., Aldwayyan, A.S.: Structural and spectroscopic studies of thin film of silver nanoparticles. Appl. Surf. Sci. **257**, 10607–10612 (2011)

Kim, S.Y., Kim, JunHo: Fabrication of CIGS thin films by using spray pyrolysis and post selenization. J. Korean Phys. Soc. **60**, 2018–2024 (2012)

Koschel, W.H., Bettini, M.: Zone-centered phonons in $A^{I}B^{III}S_2$ chalcopyrites. Phys. Stat. Sol. B **72**, 729–737 (1975)

Kotbi, A., Hartiti, B., Ridah, A., Thevenin, P.: Characteristics of $CuInS_2$ thin films synthesizes by chemical spray pyrolysis. Opt. Quantum Electron. **48**, 1–9 (2016)

Krunks, M., Mere, A., Katerski, A., Mikli, V., Krustok, J.: Characterization of sprayed $CuInS_2$ films annealed in hydrogen sulfide atmosphere. Thin Solid Films, 511–512, 434–438 (2006)

Lee, D.-Y., Kim, J.H.: Characterization of sprayed $CuInS_2$ films by XRD and Raman spectroscopy measurements. Thin Solid Films **518**, 6537–6541 (2010)

Mahendran, C., Suriyanarayanan, N.: Effect of Bi incorporation and temperature on the properties of sprayed $CuInS_2$ thin films. Phys. B **408**, 62–67 (2013)

Mahmoud, S., Eid, A.H.: Some studies on chemically and thermally prepared $CuInS_2$ films. Fiz. A **6**, 171–180 (1997)

Mott, N.F., Davis, E.A.: Conduction in non-crystalline systems V. conductivity, optical absorption and photoconductivity in amorphous semiconductors. Philos. Mag. **22**, 0903–0922 (1970)

Nakamura, S., Ando, S.: Preparation of $CuInS_2$ thin films by metal-organic decomposition. J. Phys. Chem. Solids **66**, 1944–1946 (2005)

Pankove, J.I.: Optical Processes in Semiconductors, pp. 35-46. Dover, New York (1971)

Pathan, H.M., Lokhande, C.D.: Chemical deposition and characterization of copper indium disulphide thin films. Appl. Surf. Sci. **239**, 11–18 (2004)

Rabeh, M.B., Kanzari, M.: Optical constants of Zn-doped $CuInS_2$ thin films. Thin Solid Films **519**, 7288–7291 (2011)

Rafi, M., Arba, Y., Hartiti, B., Ridah, A., Thevenin, P.: Optimization of growth of ternary $CuInS_2$ by spray pyrolysis for photovoltaic application. Moroc. J. Condens. Matter **14**, 31–35 (2012)

Reddy, T.S., Amiruddin, R., Santhosh Kumar, M.C.: Deposition and characterization of Cu_2SnS_3 thin films by co-evaporation for photovoltaic application. Solar Energy Mater. Solar Cells **143**, 128–134 (2015)

Santhosh, M.V., Deepu, D.R., Kartha, C.S., Kumar, K.R., Vijayakumar, K.P.: All sprayed ITO-free $CuInS_2$ / In_2S_3 solar cells. Solar Energy **108**, 508–514 (2014)

Sharma, A.K., Rajaram, P.: Nanocrystalline thin films of $CuInS_2$ grown by spray pyrolysis. Mater. Sci. Eng. **B 172**, 37–42 (2010)

Tang, A., Liu, J., Ji, J., Dou, M., Li, Z., Wang, F.: One-step electrodeposition for targeted off-stoichiometry Cu_2ZnSnS_4 thin films. Appl. Surf. Sci. **383**, 253–260 (2016)

Tauc, J., Menth, A.: States in the gap. J. Non-Cryst. Solids **8–10**, 569–585 (1972)

Unveroglu, B., Zangari, Giovanni: Formation of p-type CuInS2 absorber layers via sulfurization of co-electrodeposited Cu–In precursors. RSC Adv. **5**, 81642–81649 (2015)

Vadivel, S., Srinivasan, K., Murali, K.R.: Pulse electrodeposited copper indium sulfide films. Mater. Sci. Semicond. Process. **16**, 765–770 (2013)

Warren, B.E.: X-ray Diffraction. Dover, NewYork (1990)

Xu, X.H., Wang, F., Liu, J.J., Park, K.C., Fujishige, M.: A novel one-step electrodeposition to prepare single-phase $CuInS_2$ thin films for solar cells. Solid Energy Mater. Solid Cells **95**, 791–796 (2011)

Yakuphanoglu, F., Sekerci, M., Ozturk, O.F.: The determination of the optical constants of Cu (II) compound having 1-chloro-2, 3-o-cyclohexylidinepropane thin film. Opt. Commun. **239**, 275–280 (2004)

Yakuphanoglu, F., Cukurovali, A., Yilmaz, I.: Refractive index and optical absorption properties of the complexes of a cyclobutane containing thiazolylhydrazone ligand. Opt. Mater. **27**, 1363–1368 (2005)

Yeh, L.-Y., Cheng, K.-W.: Growth and characterization of $CuInS_2$ nanoparticles prepared using sonochemical synthesis. J. Taiwan Inst. Chem. Eng. **48**, 87–94 (2015)

Yukawa, T., Kuwabara, K., Koumoto, K.: Electrodeposition of $CuInS_2$ from aqueous solution (II) electrodeposition of $CuInS_2$ film. Thin Solid Films **286**, 151–153 (1996)

Zribi, M., Kanzari, M.: Effect of intentional Na-incorporation on the structural, optical and electrical properties of $CuInS_2$: Na thin films for solar energy conversion. Thin Solid Films **519**, 3865–3869 (2011)